(Letter-of-Intent to Jefferson Lab PAC 51)

GluToNγ: Gluon tomography in nucleons by γ-polarimetry

(Dated: May 21, 2023)

In this letter, we propose to measure the degree of linear polarization of a photon produced by deeply virtual Compton scattering, never considered until now as an experimental observable but rich in terms of new information about the proton structure. Indeed, the photon polarization is rigorously and straightforwardly related to the gluon transversity GPDs, still completely unknown today. This experiment would take place in the Hall C of Jefferson Lab with the NPS calorimeter coupled to a pair polarimeter specifically designed to ensure a high conversion rate and a spatial resolution good enough to resolve the small angles between the leptons.

M. Defurne[†],

DPhN (Saclay), CEA/DRF/IRFU, Gif-sur-Yvette, France

B. Wojtsekhowski,

Thomas Jefferson National Accelerator Facility, Newport News, VA 23606, USA

[†] Contact person: `maxime.defurne@cea.fr`

Contents

I. INTRODUCTION

At Jefferson Lab, a 10.6 GeV longitudinally polarized electron beam is impinged on a fixed target of liquid hydrogen to probe the proton structure. With such a beam, quarks and gluons of the valence region are under scrutiny. Thanks to the high luminosity, Jefferson Lab is able to study deep exclusive processes: a virtual photon is absorbed by the nucleon and the final state is fully characterized. These processes constrain generalized parton distributions, real functions describing the correlations between longitudinal momentum and transverse position of quarks and gluons in the proton. Being in the valence region, most of the phenomenological studies assume that only valence quarks contribute to the corresponding observables except for ϕ- and J/Ψ-meson electroproduction as strange and charm quarks are supposed to stem from fluctuations of the gluons in quark/antiquark pair. These vector mesons instantly decay and consequently allow a study of their polarization state. Although they appear very interesting from an experimental point-of-view, the validity of the factorization theorem allowing to describe the process in terms of GPDs has not been fully demonstrated yet: only amplitudes associated to the longitudinal polarization of the virtual photon at leading-order in perturbation theory can be factorized. In the case of the deeply virtual Compton scattering (DVCS) in which a high-energy photon is emitted by the quark absorbing the virtual photon, the factorization theorem has been proven valid at all orders in perturbation theory, for all polarization states of the virtual photon. Unfortunately, real photons are stable particles and are not easily delivering information about their polarization.

A. Helicity amplitudes and gluons

In deeply virtual Compton scattering (DVCS), a highly virtual photon is absorbed by the nucleon and the latter subsequently emits a high-energy real photon. At the partonic level, the process can be described by the diagrams presented in Figure 1. The process can be described in terms of helicity amplitudes $\mathcal{A}_{\mu\nu}$ being the amplitude of a virtual photon with helicity μ producing a real photon of helicity ν. Three cases must be considered:

- Helicity-conserved amplitude $\mathcal{A}_{++}$: this is a leading-twist term. Both gluons and quarks are contributing though diagram a) and b) of Figure 1. For symmetry reasons,

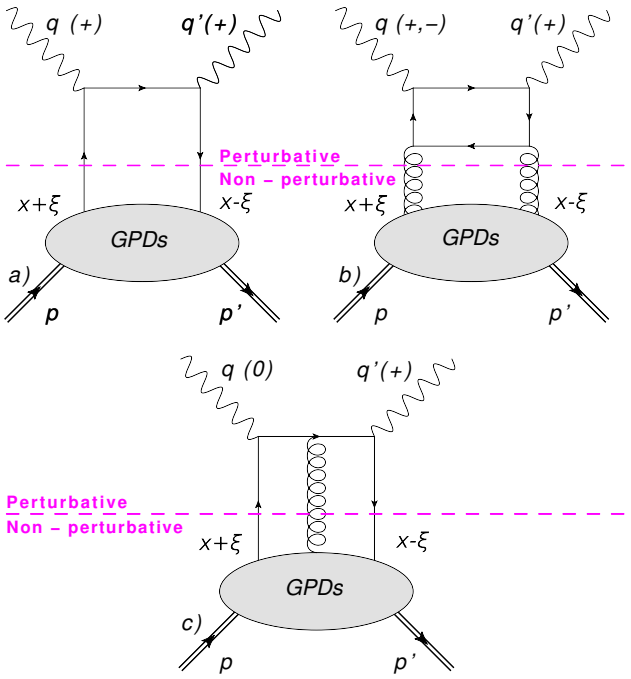

FIG. 1: The three leading-twist DVCS diagrams for all helicities of the virtual photon.

$\mathcal{A}_{++} = \mathcal{A}_{--}$. This helicity amplitude is parametrized by the chiral-even quark and gluon GPDs.

- Helicity-flip amplitude $\mathcal{A}_{0+}$: it is a twist-3 (suppressed to leading-twist) contribution described by diagram c) of Figure 1.

- Double-Helicity-flip amplitude $\mathcal{A}_{-+}$: like $\mathcal{A}_{++}$, it is a leading-twist amplitude. But **only** gluons contribute to this term through diagram b) of Figure 1.

Today, almost all phenomenological studies consider the helicity-flip amplitudes equal to 0 as not constrained. Recent pioneering phenomenological fits by the Hall A collaboration [1, 2], including kinematical power corrections to the DVCS amplitude, had to include significant contributions from the helicity-flip amplitudes. However, by lack of strong experimental evidence, their existence is still being debated in the community.

The photon polarization is an experimental measurement that will disentangle these contributions. Exact formulaes between the helicity amplitudes and the final photon polarization are currently being derived by P.A.M Guichon. For sake of simplicity/clarity in this document, we will consider $\mathcal{A}_{0+}$ null. Now assuming that we have a circularly polarized

virtual photon of helicity +, then the helicity state of the final photon λ_γ can be written:

$$|\lambda_\gamma\rangle = \sigma_{++}\,|+\rangle + \sigma_{-+}\,|-\rangle \ , \tag{1}$$

where σ_{++} (resp. σ_{-+}) will be related to $\mathcal{A}_{++}$ (resp. $\mathcal{A}_{-+}$) divided by a normalization constant. Here are the few special cases:

- if $\sigma_{-+} = 0$, then we get a perfect circularly polarized photon. In other words, it won't exhibit any linear polarization.
- if $\sigma_{-+} = -\sigma_{++}$, then we get a linearly polarized photon.
- In between these cases, the photon will be elliptically polarized. This polarization state can be described by the sum of the circularly polarized state with a fraction of linear polarization.

In other words, any degree of linear polarization in the DVCS photons will be a direct access to gluon transversity GPDs.

B. Deeply virtual Compton scattering at Next-to-leading order

Next-to-leading order (NLO) corrections to helicity-conserve CFFs have been studied in many articles such as [3]. The CFFs parametrizing the DVCS amplitude is the sum of the quark CFF and a gluon CFF, both being a convolution of the GPD with the hard scattering kerned computed at NLO. As shown on Figure 2, the quark CFF at NLO is smaller than the quark CFF computed at LO. Moreover it was found that the gluon CFF has an opposite sign compared to the quark CFF, decreasing the total CFF $\mathcal{H}$. Although model-dependent, the authors have computed a large contribution of the gluon CFF even at ξ as high as 0.2 (corresponding to $x_B \sim 0.4$) as shown by Figure 2.

NNLO corrections have been recently computed by Braun *et al.* [4]. As seen in Figure 3, NNLO corrections to quark CFFs are relatively small compared to NLO corrections. However, the gluon CFF computed at NNLO is significantly different from the NLO results. NNLO computations lead to a greater suppression of the total CFF $\mathcal{H}$ than already observed at NLO.

By sticking to a leading-order interpretation of the extracted CFFs, one may significantly underestimate the partonic content of a proton. Moreover the corrections computed in these

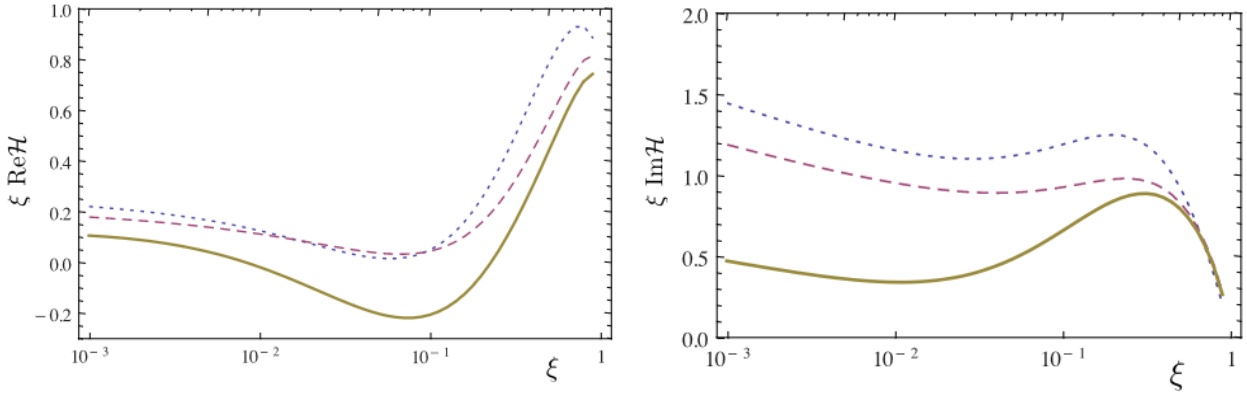

FIG. 2: Real part (Left) and Imaginary part (Right) of CFF $\mathcal{H}$ at LO (dotted line), NLO-for-quark (dashed line) and full NLO with gluons (plain line) as function of ξ at Q^2=4 GeV^2 from [3].

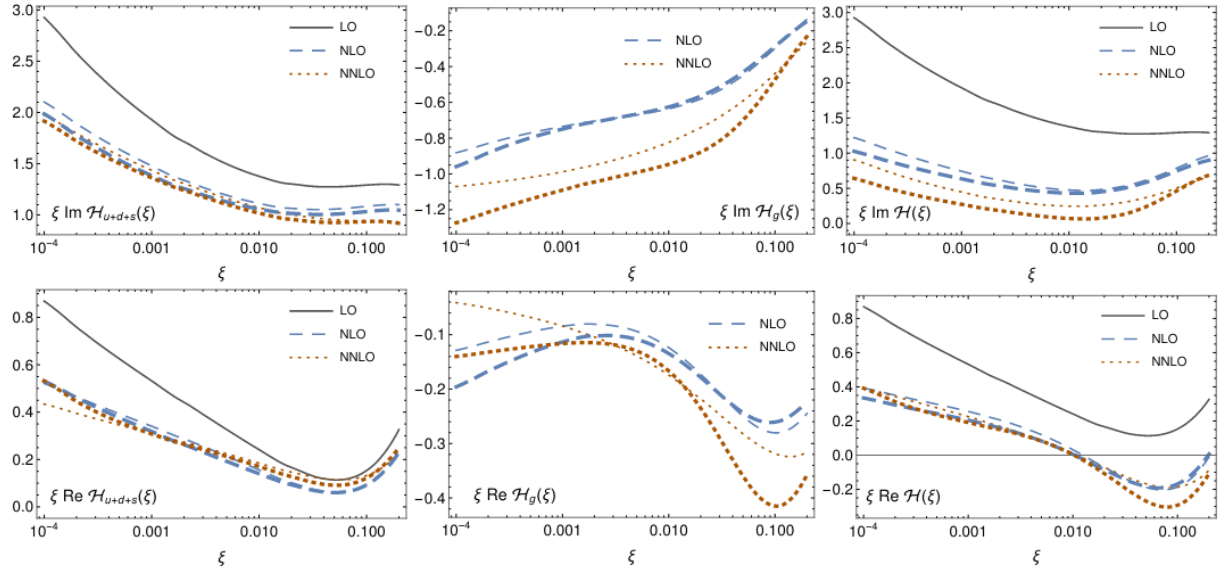

FIG. 3: Real and imaginary part of CFF $\mathcal{H}$ as a function of ξ and t=-0.1 GeV^2. The difference in the line thicknesses corresponds to different PDF normalizations for the GPD model.

studies are performed at Q^2=4 GeV^2 corresponding to a fairly large value compared to the measurements performed at Jefferson Lab.

Not much is known about chiral-even gluon GPDs by lack of clean experimental observables. Although we may hope to see a strong Q^2-dependence of the extracted CFFs, it is not clear it would happen if we consider the possible contribution of chiral-odd gluon GPDs as well in DVCS. Indeed, quarks and gluons oppose each other in the helicity-conserve amplitude whereas gluons are the only contributors to the double-helicity-flip amplitude

at leading-twist. As chiral-odd and chiral-even gluon GPDs follow the same trend with evolution, the two helicity amplitudes will have opposite trends. As they share the same kinematical coefficient in the squared DVCS amplitude on unpolarized target and are added to each other, the DVCS amplitude could remain quasi-constant while the two helicity amplitudes changes significantly. However, regarding the photon polarization, both amplitudes will be compared to each other. If we demonstrate that such a measurement is possible, it will be interesting to perform a Q^2-scan.

C. A similar study to recoil proton polarization in DVCS

Once the detailed formulaes between the helicity amplitudes and the degree of linear polarization of the photon are established, a careful study of the polarization sensitivity must be performed to choose kinematics with appropriate balance between DVCS, Bethe-Heitler and interference contributions. Based on a similar study considering the recoil proton polarization in DVCS [5], one can expect that kinematics where DVCS is dominating are to be preferred as Bethe-Heitler tends to dilute the hadronic information. Interference terms may give priviledged access to some CFFs at 90°. If confirmed, the pair polarimeter described in the next section may only need to cover a quarter or a half of the NPS calorimeter solid angle.
Regarding the contribution of the longitudinal polarization of the virtual photon, we can expect that a Rosenbluth-like measurements (same kinematics but changing the beam energy) will also constrain it.

II. A PAIR POLARIMETER FOR DVCS PHOTONS

A. Introduction to γ-polarimetry by pair production

The degree of linear polarization of photons can be derived from pair conversion of DVCS photons. As the DVCS cross section is low, the experiment is considered to be run in the Hall C of Jefferson Lab to reach a high luminosity: The electron would be detected in the HMS and the photon in NPS after going through a pair polarimeter described in subsection II D.

Upstream of this polarimeter, we consider the possibility to use the sweeping magnet in order to reduce the charged-particle background.

B. Principle and challenges of γ-polarimetry

The polarization fraction is extracted by studying the distribution of azimuthal angle ϕ of conversions. The rate is given by:

$$\frac{d\Gamma}{d\phi} \propto \left(1 + A_c P \cos\left[2\left(\phi - \phi_0\right)\right]\right) \ , \tag{2}$$

with A_c the analyzing power of the conversion, P the degree of linear polarization and ϕ_0 the angle of the polarization axis. For DVCS, the polarization axis will be defined with the kinematics of the event.

Depending on the kinematics of the DVCS reaction, the energy of the DVCS photon ranges from 2 to 8 GeV with a 10.6-GeV electron beam. For such a high-energy photon, the opening angle between the two leptons is very small. Indeed the most likely opening angle for the pair θ_{+-} is given by:

$$\theta_{+-} \sim \frac{1.6\ MeV}{E_\gamma} \ , \tag{3}$$

where E_γ is the photon energy expressed in MeV. For the DVCS energy range, θ_{+-} is between $2{\times}10^{-4}$ and $8{\times}10^{-4}$ rad. With such a low opening angle, multiple scattering can easily blur the conversion angles, dramatically reducing the analyzing power. The pair polarimeter will have to be thin to limit multiple scattering, but not too thin as the conversion rate must be high enough for the statistical significance of the measurement.

C. State-of-the-art in γ-polarimetry

γ-polarimetry is mostly used in astrophysics to caracterize the production mechanism of γ-rays in the universe (Synchrotron, Bremsstrahlung for example). Compton polarimeters are used for polarimetry up to a few MeV. But above, only pair conversion can provide information about the photon polarization. A design of pair polarimeter, for an energy going from 10 to 800 MeV, is presented in Eingorn *et al.* [6] and shown in Figure 4. The polarimeter consists of 30 cells, each made of a two double-sided micro-strip detectors (MSD) separated by 20 mm, acting as converter for the next cell and analyzers for the previous

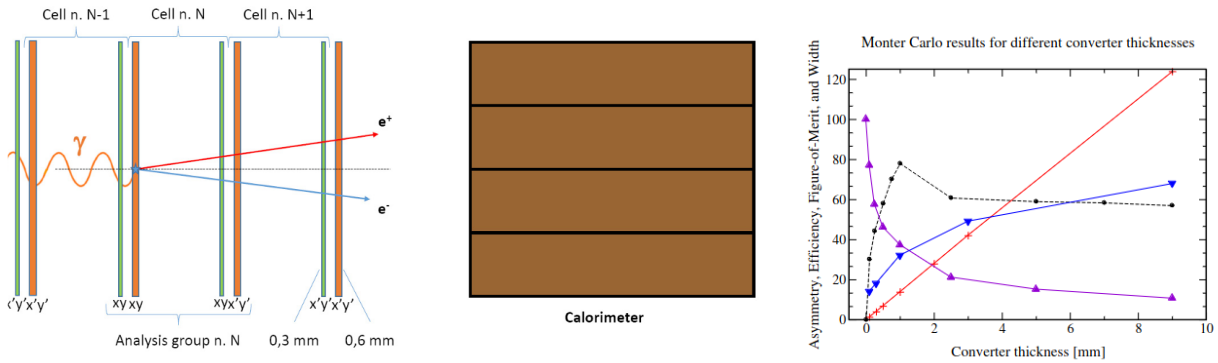

FIG. 4: Left: Schematic of the pair polarimeter. Right: Optimization of the Figure-of-merit (black line) with the converter thickness. The red line is the conversion rate, the purple line the effective analyzing power of the polarimeter and the blue line the resolution on the azimuthal angle.

cell (to determine the azimuthal angle of the lepton pair). For 500 MeV-gamma rays, the cell length must be 6.5 cm to resolve the two leptons with an accuracy good enough to measure the azimuthal angle. The radiation thickness of the MSDs was optimized such as a maximum in the Figure-of-merit is reached: While the effective analyzing power of a cell decreases with the thickness due to multiple scattering, the conversion efficiency increases more and consequently increases the Figure-of-merit until one percent of radiation length as seen in Figure 4. We are going to use this design as a start for the DVCS measurement.

D. A first concept of pair polarimeter for DVCS

To conciliate the high conversion rate and the low material budget, we consider a pair polarimeter composed of N layers of thin active radiator (t_l ~0.05% X0, ~15×15 cm^2) able to provide accurate position measurement as well, placed between the target and the NPS calorimeter. An example of detector technology able to reach such specifications are the Monolithic active pixel sensors (MAPS). The ALPIDE sensor [7] has been developped for the inner tracking system 2 of the ALICE experiment, as well as the Muon Forward Tracker. An ALPIDE sensor is 1.5 cm × 3 cm large MAPS with 512 × 1024 pixels of 28 μm × 28 μm. Figure 5 displays a matrix of 2 × 7 ALPIDE sensors.

The sensor efficiency is above 99% and the spatial resolution σ_{MAPS} was found to be better than 5 μm in [7]. However, we will remain conservative and consider σ_{MAPS}=10 μm. The silicon thickness is only 50 μm (0.05% in radiation length) but additional material

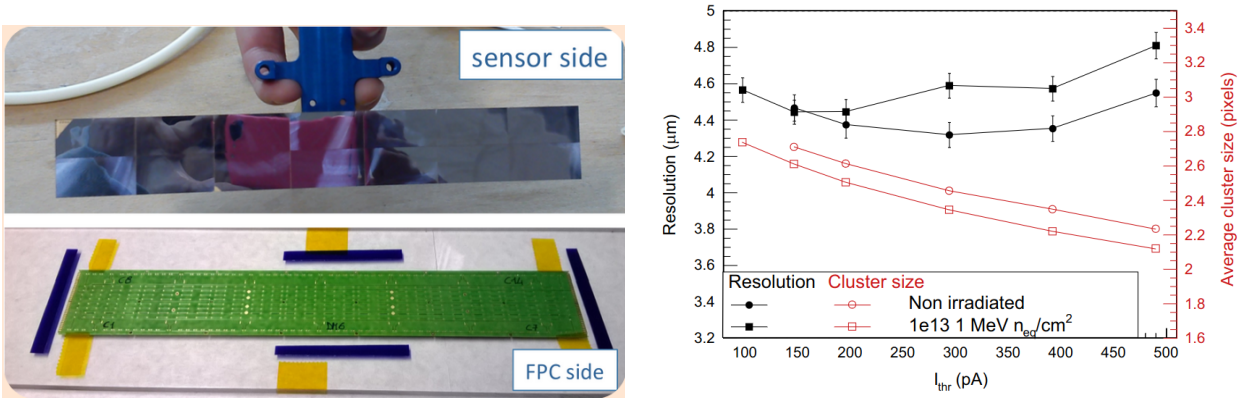

FIG. 5: Left: Pictures of ALPIDE sensors. Right: Resolution and average cluster size as function of the threshold current.

budget (0.15% in radiation length) reported for the ITS2 and the MFT systems arises from the water-based cooling system and the mechanical structure. After discussion with the technical director of the MFT system, it might not be necessary for the GluToNγ pair polarimeter to have such heavy cooling system. But as this cooling system might not super-imposed with the active area, we are going to only consider the silicon thickness. Furthermore, for the upgrade of ITS2, LHC aims at 0.05%-X0 sensors.

With a Toy Monte-Carlo simulation, we made a preliminary assessment of the performances for a pair polarimeter with the following caracteristics:

- 89 layers spaced by 0.5 cm,
- each layer with a thickness t=0.05% of radiation length,
- with a 10 μm-spatial resolution.

E. Effective analyzing power, efficiency and statistics

Multiple scattering and detector resolution will limit the accuracy on the measurement of the lepton pair plane azimuthal angle. As a result, the $\cos(2\phi)$-harmonics will be diluted and the reconstructed azimuthal distribution will read:

$$\frac{d\Gamma_{rec}}{d\phi} \propto \left(1 + A_c A_{eff} P \cos\left[2\left(\phi - \phi_0\right)\right]\right) \ , \tag{4}$$

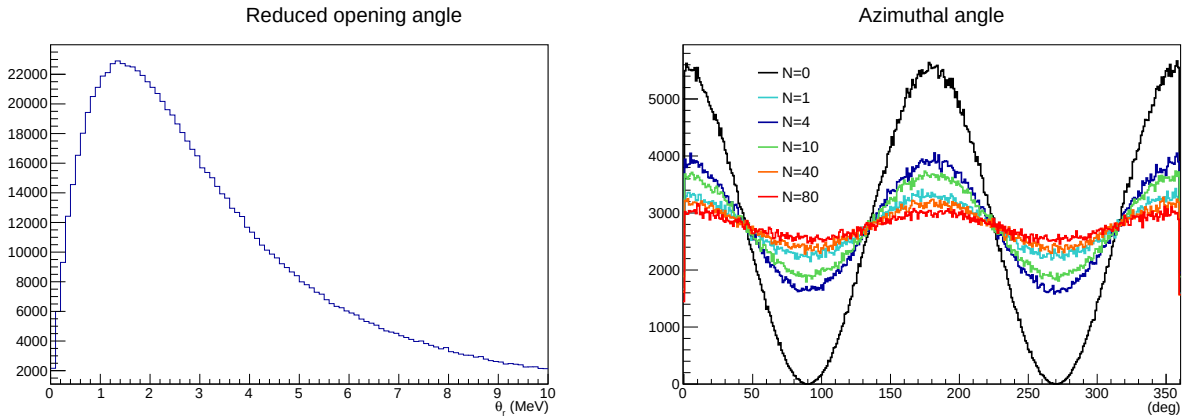

FIG. 6: Left: Generated reduced opening angle. Right: Azimuthal distribution at conversion (N=0) and measured in other layers for 2-GeV photons.

with A_{eff} the effective analyzing power of the experimental setup. For an infintely thin converter and an infintely accurate determination of the position for both leptons, A_{eff} would be equal to 1. In this Toy Monte-Carlo, we fit the azimuthal distribution at each layer (see Figure 6) obtained from the conversion of photons at layer 0 with P=1 and A_c=1, and thus for different photon energy.

As seen on Figure 7, there are two regimes:

- In the first layers, the detector resolution is limiting the analyzing power that is increasing as the distance between the two leptons is increasing.
- Then, after a given number of layers depending on the photon energy, the analyzing power start decreasing as the multiple scattering blurs the azimuthal angle at the conversion.

The overall efficiency of the polarimeter is given by $\epsilon = \eta \times \frac{1-r^n}{1-r}$ where $\eta = 1 - exp\left(-\frac{7}{9}t\right) = 3.8 \times 10^{-4}$ is the conversion rate per layer, $r = exp\left(-\frac{7}{9}t\right)$ the remaining flux of photon after a layer and n the number of convertion layers. Here the total efficiency is found to be 3.25%.

Assuming that we want to determine the degree of linear polarization of a 2-GeV DVCS photon with an accuracy of σ_P=0.1, we can derive the number of DVCS photons we would

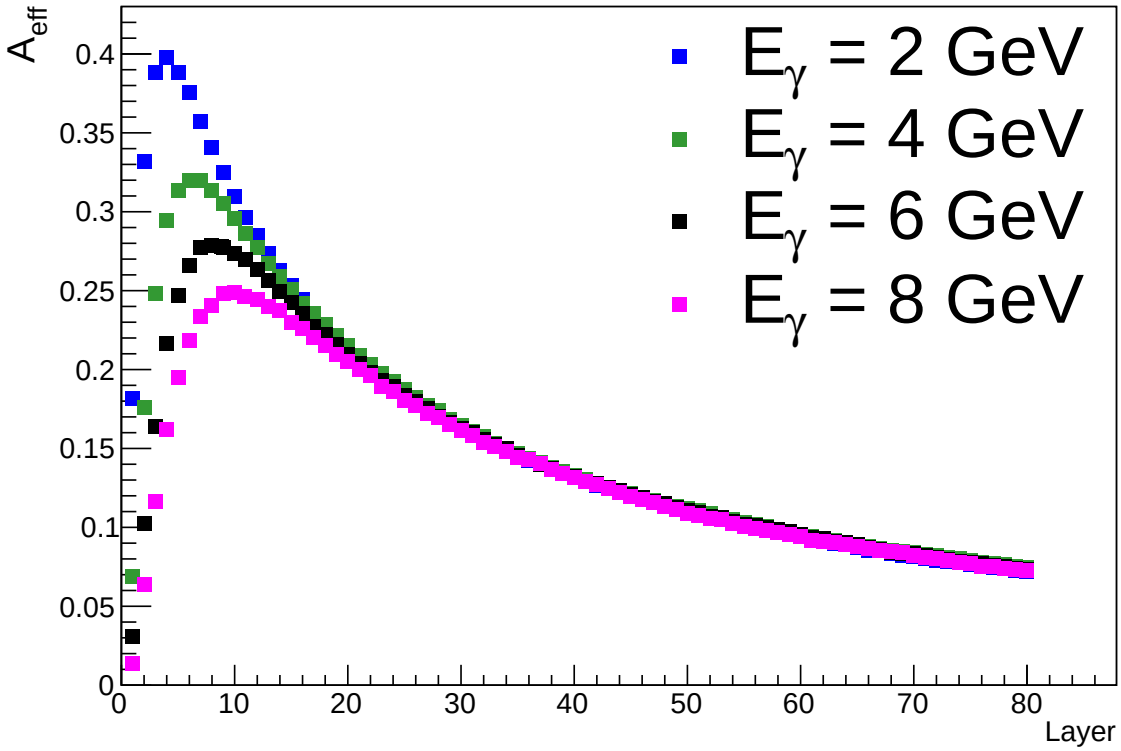

FIG. 7: Effective analyzing power as function of the layer number after the conversion. Each layer is 0.05% X0 and determine the particle position with a 10 μm-resolution

.

need as:

$$\sigma_P = \frac{1}{A_c A_{eff}} \times \sqrt{\frac{2}{\epsilon N_{DVCS}}} \rightarrow N_{DVCS} = \frac{2}{\epsilon A_c^2 A_{eff}^2 \sigma_P^2} \sim 2 \text{ Million events} \tag{5}$$

F. Discussion

The current design is just an example and not optimized at all as it was done in [6]. We want to highlight that a simultaneous optimization of several parameters must be performed all at once. For instance, the radiation length of the layers is likely too small here as we need to convert photons. If the best thickness is significantly larger than the thickness of a MAPS layer, then we must think about the geometry of the converter. Indeed a thin converter helps to determine the conversion place but an extended converter would reduce the probability of a large "multiple scattering" effect close to the conversion point and far

from the detecting MAPS layer. Finally the distance between the converter and the MAPS layer is likely to be function of the converter geometry and thickness in terms of radiation length.

Once an optimal design is found, a Geant4 simulation must be performed to determine the maximal beam current allowed by the detector rates. We do not exclude to use Super-BigBite spectrometer as electron arm to increase the acceptance of the experiment. The bin size will be adjusted with respect to the available statistics as well as the expected behaviour of the polarization with respect to the different kinematical variables.

III. CONCLUSION

In this letter-of-intent, we declare our intent to design a pair polarimeter to measure the photon linear polarization in DVCS. This observable is expected to deliver strong constrains on the elusive gluon transversity GPDs. First we are going to design a pair polarimeter optimized for photon energy ranging from 1 GeV to 4 GeV. Once the performances of the polarimeter are well caracterized, the sensitivity of the photon polarization with respect to the double-helicity-flip CFFs will be carefully studied. Finally the most suitable kinematics setting for a measurement will be determined by maximizing a figure-of-merit taking into account the DVCS cross section, the polarimeter caracteristics and the sensitivity of the polarization to the helicity-flip amplitudes.
By submitting this letter, we are looking for PAC endorsement to concretize this experiment. It will require not only simulation but also manpower and funding to build and test a prototype at a back-scattering facility once a design of pair polarimeter has been finalized.

REFERENCES

[1] M. Defurne et al. (Jefferson Lab Hall A Collaboration), Nature Communications **8**, 1408 (2017).

[2] F. Georges et al. (Jefferson Lab Hall A Collaboration), Phys. Rev. Lett. **128**, 252002 (2022), URL `https://link.aps.org/doi/10.1103/PhysRevLett.128.252002`.

[3] H. Moutarde, B. Pire, F. Sabatié , L. Szymanowski, and J. Wagner, Physical Review D **87** (2013), URL `https://doi.org/10.1103%2Fphysrevd.87.054029`.

[4] V. M. Braun, Y. Ji, and J. Schoenleber (2022), 2207.06818.

[5] O. Bessidskaia Bylund, M. Defurne, and P. A. M. Guichon, Phys. Rev. D **107**, 014020 (2023), URL https://link.aps.org/doi/10.1103/PhysRevD.107.014020.

[6] M. Eingorn, L. Fernando, B. Vlahovic, C. Ilie, B. Wojtsekhowski, G. M. Urciuoli, F. D. Persio, F. Meddi, and V. Nelyubin, Journal of Astronomical Telescopes, Instruments, and Systems **4**, 1 (2018), URL https://doi.org/10.1117%2F1.jatis.4.1.011006.

[7] M. Mager, Nuclear Instruments and Methods in Physics Research Section A: Accelerators, Spectrometers, Detectors and Associated Equipment **824**, 434 (2016), ISSN 0168-9002, frontier Detectors for Frontier Physics: Proceedings of the 13th Pisa Meeting on Advanced Detectors, URL https://www.sciencedirect.com/science/article/pii/S0168900215011122.